JOURNAL OF MAGNETIC RESONANCE, Series B **109,** 284–290 (1995)

DISTINCT NMR for Sign Determination of C–H Dipolar Couplings in Liquid-Crystalline Lipids

M. HONG* AND K. SCHMIDT-ROHR†

Materials Science Division, Lawrence Berkeley Laboratory, 1 Cyclotron Road, and Department of Chemistry, University of California, Berkeley 94720

Received April 17, 1995; revised July 5, 1995

A recently introduced DISTINCT technique for the determination of the signs of C–H dipolar couplings is described in detail. It is a switching-angle spinning experiment that employs scalar couplings to make sign-dependent heteronuclear coherence observable. The pulse sequence and the time evolution of the density operator are described, both for proton-detected local field evolution and the carbon-detected separated local field evolution. The original 1D DISTINCT experiment has also been developed into a 2D technique to allow the direct observation of antiphase dipolar powder spectra, characteristic of the signs of the dipolar couplings. These techniques are demonstrated on a liquid-crystalline lipid, lecithin.

INTRODUCTION

$^{13}C-{}^{1}H$ dipolar couplings can be powerful probes of the structure, order, and dynamics of lipids, polymers, and other organic materials. Without the need for isotopic labeling, these couplings provide information similar to that obtained by ^{2}H NMR (*1–3*). In rigid solids, the dipolar frequency for a C–H bond at an angle θ_{CH} with respect to the B_0 field is

$$\omega_d = \tfrac{1}{2}\delta_d(3\cos^2\theta_{CH} - 1),\ \delta_d = -\frac{\mu_0}{4\pi}\hbar\frac{\gamma_C\gamma_H}{r_{CH}^3}. \quad [1]$$

In uniaxial liquid crystals, motional averaging results in a dipolar frequency

$$\bar{\omega}_d = \tfrac{1}{2}\delta_d\langle 3\cos^2\Theta - 1\rangle\tfrac{1}{2}(3\cos^2\beta - 1), \quad [2]$$

where Θ denotes the angle between the C–H vector and the director (the unique motional axis) of the domain in which the segment is located, and β is the angle between the director and the B_0 field. Comparison of the two equations shows that the coupling constant of the averaged dipolar interaction, $\bar{\delta}_d$, is the product of the rigid-limit coupling constant δ_d and the C–H bond order parameter, which is the averaged term in Eq. [2],

$$\bar{\delta}_d = \tfrac{1}{2}\delta_d\langle 3\cos^2\Theta - 1\rangle. \quad [3]$$

In a dipolar Pake spectrum observed for isotropically oriented domains, this averaged coupling constant corresponds to the splitting between the two maxima. A conventional C–H dipolar spectrum is symmetric, since each orientation contributes a pair of lines at $+\bar{\omega}_d$ and $-\bar{\omega}_d$. Thus, for $|\bar{\delta}_d| \leqslant \frac{1}{2}\delta_d$, one cannot distinguish spectra arising from couplings with equal magnitude but opposite signs of $\bar{\delta}_d$. This lack of knowledge concerning the sign severely restricts the information about segmental orientation that can be drawn from $\bar{\delta}_d$. For instance, a value of $|\bar{\delta}_d| = 0.45$ can come about in many ways, while $\bar{\delta}_d = -0.45$ shows that internuclear vectors are nearly perpendicular to the director at most times. In addition to providing the average orientations of internuclear vectors, the sign of the dipolar coupling constant $\bar{\delta}_d$ is crucial for an order-tensor analysis of liquid-crystalline systems.

Traditionally, the signs of dipolar couplings have only been determined in macroscopically oriented liquid-crystalline systems (*4–7*), mostly through scaling of the dipolar couplings relative to the scalar J coupling. Recently, we have presented two switching-angle spinning (SAS) techniques that allow the determination of the sign of the C–H dipolar coupling relative to that of the J coupling in an unoriented system (*8*). Both techniques involve proton detection of local fields (PDLF) in the evolution period, a magnetization-transfer step, and ^{13}C MAS detection. The first relies on comparing the splittings found in 2D spectra with different spinning scaling factors. The second technique, called DISTINCT for *di*polar *s*ine *t*erm by *in*direct-*c*oupling *t*ransformation, uses the J coupling to make the sign-dependent sine term of the dipolar coherence observ-

* To whom correspondence should be addressed.

† Present address: Department of Polymer Science and Engineering, University of Massachusetts, Amherst, Massachusetts 01003.

1064-1866/95 $12.00

able. The sign of the dipolar coupling is eventually manifested as the sign of the ^{13}C peak intensity in a 1D spectrum.

In this paper, we describe the DISTINCT technique in detail. The time evolution of the density operator will be presented. We show, both theoretically and experimentally, that the intensities of ^{13}C signals are mainly determined by the 90° singularities of the dipolar powder spectrum. From 2D DISTINCT spectra, the sign of the averaged dipolar constant can be determined unambiguously. In practice, the sign determination is most reliable when the scaled dipolar coupling is larger than the J coupling. We also discuss a variation of the 1D DISTINCT experiment which begins with ^{13}C magnetization in the evolution period.

EXPERIMENTAL CONDITIONS

Lecithin (a phosphatidylcholine) is a lipid abundant in biological membranes. It was chosen in this study because ^{2}H quadrupolar couplings have been measured for more than 20 sites (*1, 9*) in this molecule and can be used as a reference for the dipolar couplings. The lipid in powder form was purchased from Avanti Polar lipids (Alabaster, Alabama), and hydrated in D_2O at 70/30 (w/w) after several freeze–thawing cycles to obtain a uniform aqueous dispersion.

The experiments were carried out on a homebuilt 7.07 T spectrometer with a Tecmag pulse programmer and data-acquisition system. The sample was spun at about 2 kHz using a Doty Scientific 7 mm spinner in a homebuilt SAS probehead (*10*). The orientation of the rotor axis was controlled by a stepping motor attached to the bottom of the probe and a computerized motor controller with an angular precision of 0.2°. The hopping time for the rotor was less than 60 ms. ^{1}H and ^{13}C RF field strengths of about 50 kHz were used. The MREV-8 cycle time of 120 μs was one quarter of the sample-rotation period t_r.

DISTINCT WITH ^{1}H-DETECTED LOCAL-FIELD EVOLUTION

The DISTINCT pulse sequence is displayed in Fig. 1. In the evolution period, the sample is spun off the magic angle (OMAS) so that all anisotropic interactions are scaled by $P_2(\cos\theta) = \frac{1}{2}(3\cos^2\theta - 1)$, where θ is the angle between the rotor axis and the B_0 field (*11*). By homonuclear proton decoupling and simultaneous ^{1}H (I-spin) and ^{13}C (S-spin) 180° pulses that refocus the chemical-shift interaction, only C–H heteronuclear interactions are retained. These include the C–H dipolar coupling, which is scaled by $P_2(\cos\theta)$ and the MREV-8 scaling factor s_m, and the isotropic J coupling. The anisotropic part of the J coupling can be neglected relative to the dipolar coupling (*12*). The initial proton magnetization I_y, created by a 90° x pulse, thus evolves under the averaged heteronuclear Hamiltonian

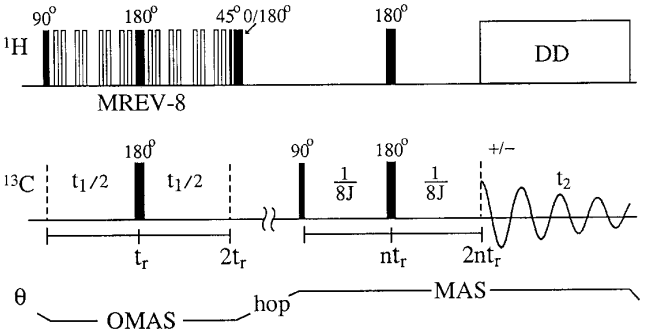

FIG. 1. DISTINCT pulse sequence for the sign determination of C–H couplings by detection of sine-modulated heteronuclear coherence. During the evolution time, the sample is spun at $\theta \neq 54.74°$, and MREV-8 decoupling and simultaneous 180° pulses are applied to remove all interactions except for the heteronuclear coupling. Under this coupling, the ^{1}H magnetization evolves into sine-modulated heteronuclear coherence, which is then converted into two-spin order S_zI_z by a 45° pulse at the end of the evolution time. The 45° pulse is followed by two proton 90° pulses, which are phase-cycled to effectively make up a pair of 0° and 180° pulses to remove the direct ^{13}C magnetization. The sample is then hopped to the magic angle. In the ensuing J-coupling period, the dipolar couplings are refocused at full rotor periods while 180° pulses refocus the chemical shift. By means of a 90° ^{13}C pulse and the rotor-synchronized J-coupling period, the two-spin order is transformed into observable ^{13}C magnetization, which is detected under proton decoupling. ^{1}H and ^{13}C 90° pulse lengths range from 6 to 9 μs, depending on the spinner orientation.

$$H_{CH} = s_m(P_2(\cos\theta)\bar{\omega}_d + \pi J)2S_z\frac{1}{\sqrt{2}}(I_z + I_x) \quad [4]$$

into heteronuclear coherence according to

$$I_y \rightarrow I_y\cos(\omega_{CH}t_1) + 2S_z\frac{1}{\sqrt{2}}(-I_x + I_z)\sin(\omega_{CH}t_1), \quad [5a]$$

where

$$\omega_{CH} = s_m(P_2(\cos\theta)\bar{\omega}_d + \pi J) \quad [5b]$$

and $\bar{\omega}_d$ and J are the dipolar and the spin–spin couplings of a proton to its directly bonded carbon. At the end of the evolution period, a ^{1}H $45°_{-y}$ pulse converts the sine component in Eq. [5a] into two-spin order $2S_zI_z\sin(\omega_{CH}t_1)$, whereas the I_y term remains invariant. During the subsequent hop of the sample rotor to the magic angle, the transverse magnetization I_y dephases while the two-spin order survives. This two-spin order is then transformed into heteronuclear coherence $2S_xI_z\sin(\omega_{CH}t_1)$ by means of a carbon $90°_{-y}$ pulse after the hop.

In the next time period of length $\tau = 2nt_r$, all interactions are removed except for the isotropic J coupling: the chemi-

cal-shift interaction is refocused by ^{1}H and ^{13}C 180° pulses at $\tau/2$, while the C–H and the H–H dipolar couplings are averaged out at full MAS rotor periods nt_r due to the uniaxial motional averaging in the lipid system (*13, 14*). This J interaction transforms the heteronuclear coherence $2S_xI_z$ into observable ^{13}C magnetization S_y, which is finally detected under proton decoupling. The last transformation is given by

$$2S_xI_z \rightarrow 2S_xI_z\cos(\pi J\tau) + S_y\sin(\pi J\tau) \qquad [6]$$

for a CH group. In general, for a CH_n ($n = 1, 2, 3$) segment that contains one ^{13}C nucleus evolving in the sum fields of n protons, the observed density operator is

$$S_y\sin(\omega_{CH}t_1)\sin(n\pi J\tau) \qquad [7]$$

for methine ($n = 1$) and methylene groups ($n = 2$). (An analogous calculation is outlined in the section ''DISTINCT by ^{13}C-Detected Local Field'' below.) For methyl groups, the signal is

$$S_y\sin(\omega_{CH}t_1)[\sin(3\pi J\tau) + \sin^3(\pi J\tau)]. \qquad [8]$$

Since CH_2 groups are predominant in the lipid molecule, the length of the J-coupling period in our experiments was chosen as $\tau = 1/4J$ so that $\sin(2\pi J\tau) = 1$ to maximize the signal. Thus during detection, one obtains ^{13}C MAS signals that are modulated by the sine of the heteronuclear C–H couplings:

$$f(t_1, t_2) \propto \sin(\omega_{CH}t_1)\exp(i\omega_{cs}t_2). \qquad [9]$$

At sufficiently short t_1, due to

$$\sin(\omega_{CH}t_1) \approx \omega_{CH}t_1, \qquad [10]$$

the sign of the heteronuclear coupling ω_{CH} is manifested as the sign of the ^{13}C MAS signal. It can be directly converted into the sign of the dipolar coupling $\bar{\omega}_d$, provided that the scaled dipolar coupling is larger than the J coupling, i.e., $P_2(\cos\theta)\bar{\omega}_d > \pi J$.

EFFECTS OF THE POWDER AVERAGE

Up to this point, we have neglected the fact that the dipolar spectrum for our multidomain liquid-crystalline sample is a powder pattern rather than a single pair of lines (*15*). One might suspect that such a distribution of frequencies in the dipolar pattern, which results in varying signs of $P_2(\cos\beta)$ in Eq. [2], makes the sign of the dipolar frequencies ω_{CH} indeterminate. However, this is not the case. A sine-modulated dipolar powder spectrum (Fig. 2a) is dominated by singularities at

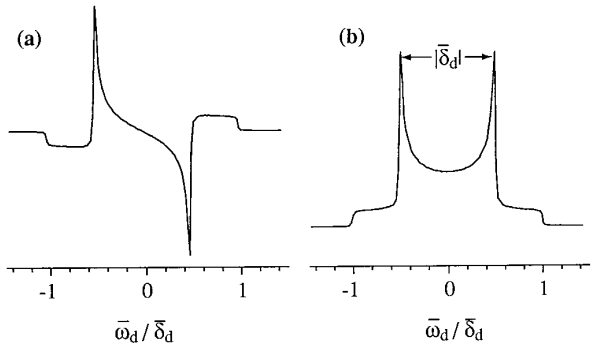

FIG. 2. Simulation of antiphase and in-phase powder spectra of dipole coupling resulting from sine and cosine time evolution, respectively. (a) The antiphase spectrum is antisymmetric with respect to $\bar{\omega}_d = 0$. Depending on the sign of $\bar{\delta}_d$, the polarity of the spectrum changes. (b) The in-phase spectrum (Pake pattern). The two transitions are symmetric with respect to $\bar{\omega}_d = 0$. Spectra with the same $|\bar{\delta}_d|$, but different signs of $\bar{\delta}_d$, are indistinguishable. In these spectra, for simplicity, the J coupling was neglected and all scaling factors were set to unity.

$$\pm\omega_{CH}(\beta = 90°) = \pm s_m(-\tfrac{1}{2}\bar{\delta}_d P_2(\cos\theta) + \pi J), \qquad [11]$$

which correspond to bilayers whose directors are perpendicular to the magnetic field. The ^{13}C MAS signals in the 1D DISTINCT spectra are mainly modulated by these powder maxima and thus should reflect the opposite sign of the averaged dipolar coupling $\bar{\delta}_d$ due to $P_2(\cos 90°) < 0$. Note that the sine powder pattern is antisymmetric and can be described as $P(\omega - \pi J) - P(-\omega + \pi J)$, where $P(\omega)$ is the lineshape function for a single transition, while the conventional cosine Pake pattern (Fig. 2b) is symmetric with a lineshape of $P(\omega - \pi J) + P(-\omega + \pi J)$. Due to this antisymmetry, the ''polarity'' of the sine dipolar spectrum changes according to the sign of $\bar{\delta}_d$ (provided that the scaled dipolar coupling exceeds the J coupling).

To verify that the dipolar powder maxima indeed determine the ^{13}C MAS intensity, one can increment t_1 in the DISTINCT pulse sequence to obtain a 2D spectrum, in which the ω_1 dimension explicitly shows the antiphase spectra of the C–H dipolar coupling.

The expected antiphase powder spectra depend on the signs and relative sizes of J and dipolar couplings, as shown in Fig. 3. Here the sign of the J coupling is set to be positive, as appropriate for one-bond couplings. The spectra consist of two halves of a Pake pattern, $\pm P[\pm(\omega - \pi J)]$, each of width $1.5P_2(\cos\beta)\bar{\delta}_d$, with centers of gravity at $\pm\pi J$. The polarity of the spectral maxima, which is the most easily detected feature, changes at parameter values of $P_2(\cos\theta)\bar{\delta}_d = +\pi J$. As expected, for dipolar couplings of magnitude

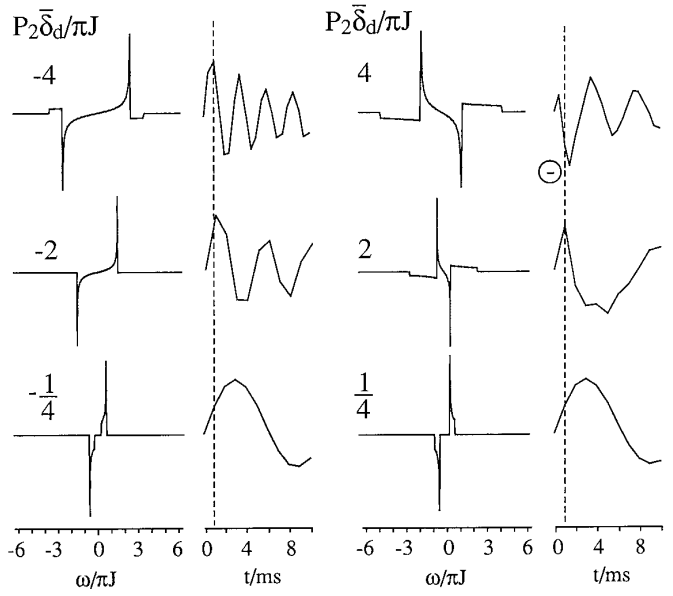

FIG. 3. Simulation of the antiphase dipolar powder spectra with J coupling, and their corresponding time-domain sine oscillations as a function of $P_2(\cos\theta)\bar{\delta}_D/\pi J$, where θ is the angle of the spinner axis with respect to the external field. When $|P_2\bar{\delta}_D| \gg \pi J$ (e.g., the ratio is 4), the initial intensity of the time signal is sensitive to the sign of the dipolar coupling constant. For $|P_2\bar{\delta}_D| \leqslant \pi J$ (e.g., the ratios are 2 and $\frac{1}{4}$), the beginning of the time signal is dominated by the slow oscillation of the J coupling and is invariant to the sign of $\bar{\delta}_D$. The dashed line indicates the fixed t_1 time of ~2 ms used in our 1D DISTINCT experiments. In the spectral patterns, note the switch of polarity around $P_2\bar{\delta}_D/\pi J = +1$. The spectra for very small dipolar couplings of equal magnitude but opposite signs (e.g., $P_2\bar{\delta}_D/\pi J = \pm\frac{1}{4}$) have the same polarity but different lineshapes.

smaller than the J coupling, the polarity is that of an antiphase J doublet. However, Fig. 3 shows that, even for these small dipolar couplings, the details of the powder patterns are different. As shown in the examples of $P_2\bar{\delta}_D/\pi J = \pm 1/4$, the relative positions of the maxima and the low edges of the powder spectra make it possible to determine the sign and magnitude of the dipolar coupling, provided the resolution is sufficient.

Figure 4 shows the experimental 2D DISTINCT spectrum of lecithin with a spinning scaling factor of $P_2(\cos\theta) = -0.2$. The signals of the different molecular sites are separated in the ω_2 dimension according to the ^{13}C isotropic chemical shift. In the ω_1 dimension, the heteronuclear spectra of individual sites exhibit positive and negative intensities that are antisymmetric with respect to $\omega_1 = 0$. The largest intensities in each cross section occur at $\pm s_m(-\frac{1}{2}\bar{\delta}_d P_2(\cos\theta) + \pi J)$, corresponding to the 90° orientation of the bilayer normal with respect to the B_0 field. The fact that the polarities of the antiphase patterns in the 2D spectrum are the same except for that of C_α indicates that all sites except for C_α have the same sign for the couplings ω_{CH}. The structural implication for the sign change of the C_α–H coupling will be mentioned below.

The 2D spectrum strongly suggests that the ^{13}C signals in the 1D DISTINCT spectra reflect the sign of the dipolar coupling $\omega_{CH}(\beta = 90°)$ at the singularities of the powder pattern. For a more complete analysis of the 1D DISTINCT intensities, one needs to examine the time-domain oscillations of the antiphase heteronuclear spectra, as the ^{13}C signals are modulated by $\sin(\omega_{CH}t_1)$ [9]. In addition, the effect of the positive $^1J_{CH}$ coupling on the sign determination must be included. The sine-time signals corresponding to the antiphase spectra for a series of relative ratios of the dipolar and J couplings are shown in Fig. 3. The behavior of the signals at long and intermediate times is clearly dominated by the oscillation of the 90° frequencies. The behavior at

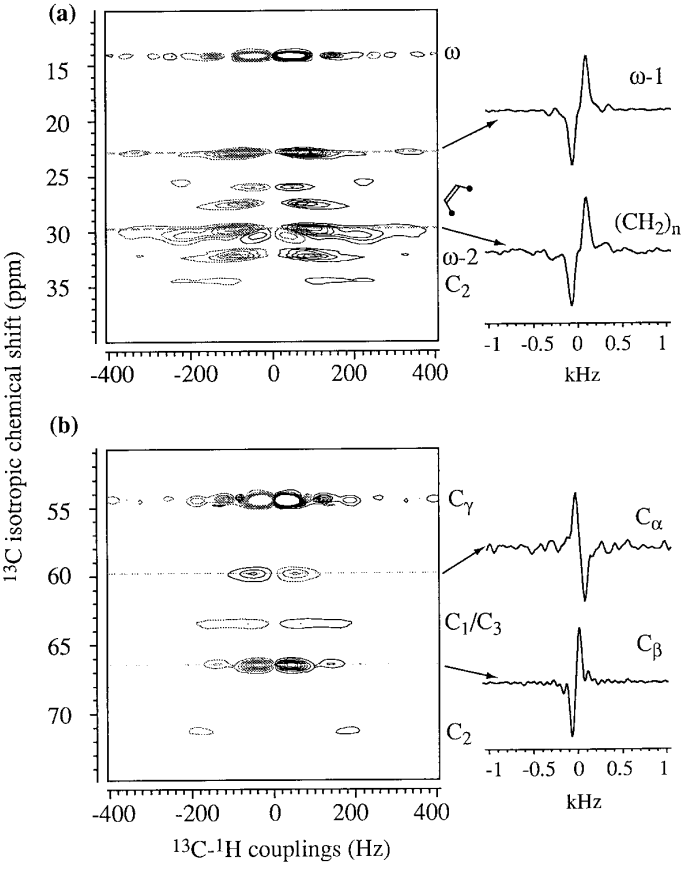

FIG. 4. Two-dimensional DISTINCT spectrum of lecithin in the L_α phase, taken with a spinning scaling factor of $P_2(\cos\theta) = -0.2$. (a) Acyl chain region. (b) Headgroup and glycerol regions. The antiphase spectra of the C–H couplings in ω_1 are antisymmetric, indicated by negative (gray) and positive (black) intensities. Several cross sections of C–H coupling are shown on the side. The 90° singularities exhibit the strongest intensities in these powder patterns. The spectrum shows that the sign of the C_α–H coupling is opposite to those of other segments. The measuring time was 10 h.

short and intermediate times, which are of most interest to 1D DISTINCT experiments, can be written as

$$f_s(t) = \int P(\omega)\sin(\omega t)d\omega$$
$$= t\int P(\omega)\omega d\omega - \frac{t^3}{6}\int P(\omega)\omega^3 d\omega + O(t^5)$$
$$= -\frac{t^3}{6}M_3 + O(t^5) \qquad [12]$$

for the case without J coupling. The first moment $\int P(\omega)\omega d\omega$ vanishes since it corresponds to the center of gravity of $P(\omega)$, and the third moment M_3 has the same sign as $\overline{\delta}_d$. When J coupling is present, the signal at short times becomes

$$f_s(t) = t\pi J - \frac{t^3}{6}M_3 + O(t^5). \qquad [13]$$

This means that when the P_2-scaled dipolar coupling is comparable to the J coupling constant, i.e., when the first term in [13] is greater than the second term, the signal at short times fails to reflect the sign of $\overline{\delta}_d$. As indicated in Fig. 3, the initial decays of the time signals with $P_2(\cos\theta)\overline{\delta}_d \gg \pi J$ (the ratios of ± 4 being an example) are sensitive to the 90° singularities of the dipolar spectra. The signal at a fixed initial time point (1 ms) changes sign with the sign of the dipolar coupling. However, when $P_2(\cos\theta)\overline{\delta}_d \leqslant 2\pi J$ (the ratios of ± 2 and ± 0.25 are examples), the time signal remains positive at the beginning, since it does not oscillate fast enough to reflect the 90° frequency of the powder pattern. Thus, the 1D DISTINCT experiment is able to detect the sign only for relatively large dipolar couplings. Fortunately, in phosphatidylcholine, the dipolar couplings of most headgroup and glycerol sites of interest are much larger than the isotropic J coupling, as suggested by the ^{2}H NMR data. Additionally, the signs of small dipolar couplings can be determined by other techniques such as 2D PDLF NMR (*8*).

To demonstrate the technique, two 1D DISTINCT spectra of lecithin taken at $P_2(\cos\theta) = \pm 0.2$ are displayed in Fig. 5. The evolution time was chosen to be 960 μs, which corresponds to two rotor periods, to maximize the signal. In both spectra, the sign of the CH_3 (ω and γ site) signals (*16*) provides the positive reference, since in these groups the positive one-bond J coupling (*12*) dominates the weak dipolar couplings. It follows that negative signal intensities in either spectrum are definite indications that the P_2-scaled dipolar coupling constant has the same sign as the J coupling, and that $P_2(\cos\theta)\overline{\delta}_d \gg \pi J$ (Fig. 4). For example, at

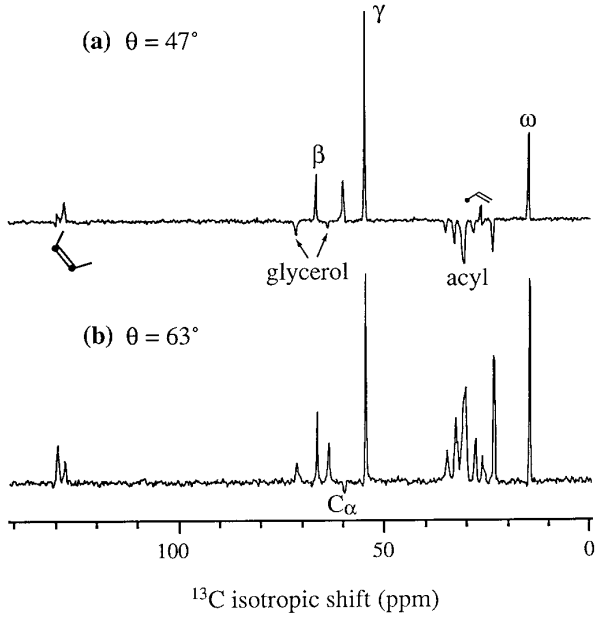

FIG. 5. One-dimensional DISTINCT spectra of L_α lecithin at spinning scaling factors (a) $P_2 = +0.2$ and (b) $P_2 = -0.2$. The sign of each peak reflects the sign of the sum of the corresponding J coupling and P_2-scaled dipolar coupling constant. Negative peaks at $P_2 = +0.2$ indicate large positive dipolar coupling constants, while the negative C_α peak at $P_2 = -0.2$ demonstrates that its $\overline{\delta}_d$ is negative. The assignment of the ^{13}C MAS signals are made according to Husted *et al.* (*16*). Measuring times were 8 and 4 h.

$P_2(\cos\theta) = +0.2$, the acyl carbons exhibit negative signals, so the dipolar coupling constant $\overline{\delta}_d$ of acyl sites is positive. Taking into account that the rigid-limit dipolar constant δ_d is *a priori* negative [1], we conclude that the acyl carbons have a negative order parameter $S = \frac{1}{2}\langle 3\cos^2\Theta - 1\rangle$. This is consistent with the parallel orientation of the acyl chains with the bilayer normal, since the C–H vectors are preferentially perpendicular to the director and the corresponding $\frac{1}{2}\langle 3\cos^2\Theta - 1\rangle$ term is negative. Carrying out the same analysis for the spectrum taken at $P_2(\cos\theta) = -0.2$, in which all sites except C_α exhibit positive signals, we find that C_α is the only segment with a large positive order parameter or a large negative coupling constant $\overline{\delta}_d$. This demonstrates an unusual orientation of the C_α methylene group, which is consistent with the bend of the lipid molecule at the phosphate junction (*17*).

Comparing the merits of 1D and 2D DISTINCT spectroscopy, it is clear that the 1D technique permits a quicker examination of the signs of dipolar couplings. However, the interpretation of the 1D spectra can be ambiguous due to the above-mentioned complex time evolution for a powder sample, especially when the dipolar couplings are small compared to the J coupling. Therefore, the 2D version of DISTINCT, while more time consuming, is important for a clear final determination of the signs of the dipolar couplings.

DISTINCT BY ^{13}C-DETECTED LOCAL FIELD

The DISTINCT technique can also be implemented beginning with ^{13}C magnetization that evolves in the fields of the surrounding protons, as in conventional separated-local-field (SLF) experiments (*18, 19*). Since n protons interact with the ^{13}C spin in a CH_n (n = 1, 2, 3) segment, the ^{13}C MAS signal is modulated by the sine of the *sum* of the C–H dipolar couplings. This can be derived by considering the Hamiltonian for the interaction of protons a, b, . . . with the ^{13}C spin

$$H_{CH} = 2S_z(\omega^a_{CH}I^a_z + \omega^b_{CH}I^b_z + \ldots), \qquad [14]$$

where it has been taken into account that the tilting of the MREV-8 toggling frame is corrected by a ^{1}H $45°_{-y}$ pulse at the end of the evolution period. In the Hamiltonian [14], the coupling terms for spins $a, b, \ldots$ commute. Therefore, the time evolution can be calculated by successive evaluation of their effects on the density operator (*20*). For a CH_2 group, the density operator is found to evolve under the dipolar Hamiltonian as

$$\begin{aligned} S_y \xrightarrow{t_1} & 2S_xI^a_z \sin(\omega^a_{CH}t_1)\cos(\omega^b_{CH}t_1) \\ & + 2S_yI^b_z\cos(\omega^a_{CH}t_1)\sin(\omega^b_{CH}t_1) \\ \xrightarrow{\tau} & S_y[\sin(\omega^a_{CH}t_1)\cos(\omega^b_{CH}t_1) \\ & + \cos(\omega^a_{CH}t_1)\sin(\omega^b_{CH}t_1)] \\ & \times \sin(\pi J\tau)\cos(\pi J\tau), \end{aligned} \qquad [15]$$

where only the relevant terms are given. The frequencies ω^a_{CH} and ω^b_{CH} are the heteronuclear couplings of the carbon to protons a and b, respectively. Note that the signal [15] has the required invariance with respect to an interchange of protons a and b. The detected signal after J evolution under MAS can be rewritten as

$$\begin{aligned} & S_y\sin\{s_m[P_2(\cos\theta)\cdot(\omega^a_d + \omega^b_d) + 2\pi J]t_1\} \\ & \times \tfrac{1}{2}\sin(2\pi J\tau). \end{aligned} \qquad [16]$$

As before, in order to obtain maximal ^{13}C signals, τ is chosen such that $\sin(2\pi J\tau) = 1$.

Two SLF-DISTINCT spectra are shown in Fig. 6, with scaling factors of $P_2(\cos\theta) = \pm 0.2$. The signs of all peaks in each spectrum are consistent with those obtained in the corresponding PDLF spectrum (Fig. 5). ^{2}H NMR and our 2D PDLF spectra (*8*) have shown that the two C–H couplings, ω^a_d and ω^b_d, are degenerate in most CH_2 groups of lecithin. As a result, the ^{13}C signals are modulated by approximately twice the C–H coupling observed in the corresponding PDLF spectrum. This difference in the modulation frequency gives rise to different intensity ratios in the SLF- and PDLF-DISTINCT spectra. For instance, at $P_2(\cos\theta) = +0.2$, the γ peak in Fig. 6 is 8 times higher than the main $(CH_2)_n$ peak, while the ratio is only about 5 in the corresponding PDLF spectrum. Clearly, the ^{13}C-detected DISTINCT spectra have a lower sensitivity, which is mostly due to the scaling of the overall signal by the factor of $\frac{1}{2}$ in Eq. [16] compared to the PDLF signal (Eq. [7]). Consistently, the S/N is similar for the C–H signals (near 130 ppm), since C–H groups evolve identically under SLF and PDLF conditions.

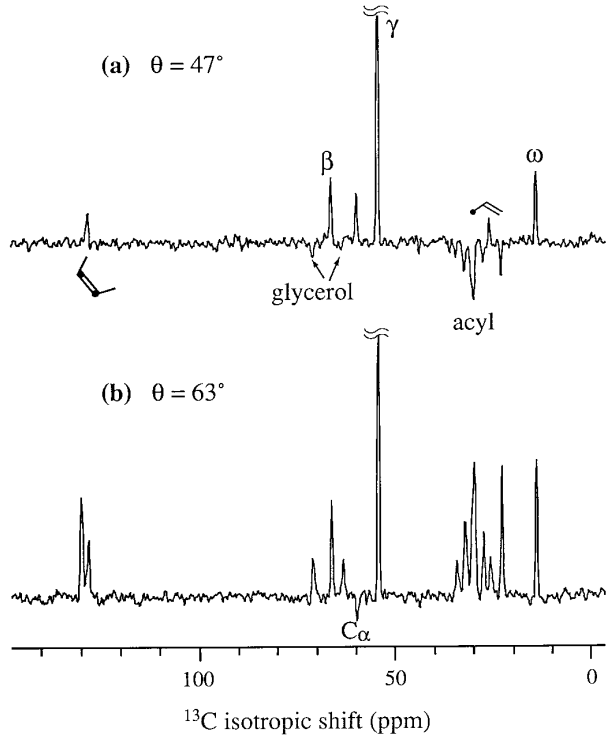

FIG. 6. One-dimensional DISTINCT spectra of lecithin starting with ^{13}C magnetization. (a) $P_2 = +0.2$. (b) $P_2 = -0.2$. The measuring time was 8 h for each spectrum.

CONCLUSIONS

The DISTINCT technique described here allows us to determine the signs of heteronuclear dipolar couplings between J-coupled ^{13}C and ^{1}H nuclei in lipids. The method is quite direct, allowing the observation of the signs of dipolar couplings in terms of ^{13}C 1D MAS signals or via the polarities of signals in the 2D version of the DISTINCT experiment. To understand the effect of the powder averaging on the 1D DISTINCT signals, we considered the time signals

at short and intermediate times. The 1D DISTINCT experiment is an attractive method for a relatively quick examination of the signs of dipolar couplings in motionally averaged systems such as liquid crystals. It does not work well for dipolar couplings smaller than the J coupling; however, it is quite independent of the MREV-8 scaling factor, in contrast to methods for sign determination based on analyzing dipolar splittings at different spinning angles.

ACKNOWLEDGMENTS

This work was supported by the Director, Office of Energy Research, Office of Basic Energy Sciences, Materials Science Division of the U.S. Department of Energy under Contract DE-AC03-76SF00098. We are grateful to Professor Alexander Pines for his advice and encouragement of this work. K.S.-R. acknowledges a fellowship from the BASF AG and the German National Scholarship Foundation.

REFERENCES

1. J. Seelig and A. Seelig, *Q. Rev. Biophys.* **13,** 19 (1980).
2. H. W. Spiess, *Adv. Polym. Sci.* **66,** 23 (1985).
3. J. Seelig, P. M. Macdonald, and P. G. Scherer, *Biochemistry* **26,** 7535 (1987).
4. B. M. Fung, A. Jalees, T. L. Foss, and M.-H. Chau, *J. Chem. Phys.* **85,** 4808 (1986).
5. P. Diehl and C. L. Khetrapal, *NMR: Basic Princ. Prog.* **1,** 1 (1969).
6. C. R. Sanders and J. H. Prestegard, *J. Am. Chem. Soc.* **113,** 1987 (1991).
7. C. R. Sanders, B. J. Hare, K. P. Howard, and J. H. Prestegard, *Prog. NMR Spectrosc.* **26,** 421 (1994).
8. M. Hong, K. Schmidt-Rohr, and A. Pines, *J. Am. Chem. Soc.* **117,** 3310 (1995).
9. P. G. Scherer and J. Seelig, *Biochemistry* **28,** 7723 (1989).
10. M. A. Eastman, P. J. Grandinetti, Y. K. Lee, and A. Pines, *J. Magn. Reson.* **98,** 333 (1992).
11. M. Mehring ''High Resolution NMR in Solids,'' Springer-Verlag, New York, 1983.
12. C. J. Jameson, *in* ''Multinuclear NMR'' (J. Mason, Ed.), Plenum Press, New York, 1987.
13. J. Forbes, C. Husted, and E. Oldfield, *J. Am. Chem. Soc.* **110,** 1059 (1988).
14. M. M. Maricq and J. S. Waugh, *J. Chem. Phys.* **70,** 3300 (1979).
15. U. Haeberlen, ''High Resolution NMR in Solids Selective Averaging,'' Academic Press, New York, 1976.
16. C. Husted, B. Montez, C. Le, M. A. Moscarello, and E. Oldfield, *Magn. Reson. Med.* **29,** 168 (1993).
17. J. Seelig, H.-U. Gally, and R. Wohlgemuth, *Biochim. Biophys. Acta* **467,** 109 (1977).
18. R. K. Hester, J. L. Ackermann, B. L. Neff, and J. S. Waugh, *Phys. Rev. Lett.* **36,** 108 (1976).
19. E. F. Rybaczewski, B. L. Neff, J. S. Waugh, and J. S. Shefinski, *J. Chem. Phys.* **67,** 1231 (1977).
20. R. R. Ernst, G. Bodenhausen, and A. Wokaun, ''Principles of Nuclear Magnetic Resonance in One and Two Dimensions,'' Clarendon Press, Oxford, 1987.